

Multi-nucleon correlations in Deep Inelastic Scattering at large Bjorken x_B

Alberto Accardi^a, Jian-Wei Qiu^{a,b} and James P. Vary^a

^a*Department of Physics and Astronomy, Iowa State University, Ames, IA 50011-3160, U.S.A.*

^b*Physics Department, Brookhaven National Laboratory, Upton, NY 11973-5000, U.S.A.*

(Dated: January 10, 2007)

Using realistic nuclear many-body wave functions in the collinear factorization framework, we evaluate nuclear Deep Inelastic Scattering at large Bjorken x_B , where correlations are needed to exceed the kinematic limits of a single free nucleon. We find that recent experimental data on cross-section ratios from the CLAS collaboration exhibit features that are not reproduced by modern 2- and 3-nucleon correlations in the nuclear wave function. New physical mechanisms are needed to explain data in the $2 \lesssim x_B \lesssim 3$ range.

PACS numbers: 12.38.Bx, 13.60.Hb, 21.30.-x, 24.85.+p

Keywords: two- and three-nucleon correlations, scaling at large x_B , collinear factorization

Introduction. The CLAS collaboration has recently published data on ratios of cross-sections for scattering a high-energy electron on a nucleus A to ${}^3\text{He}$ at large $x_B < 3$ [1, 2]. These ratios show an interesting structure with 2 plateaus at $x_B \gtrsim 1.5$ and $x_B \gtrsim 2.25$, of height increasing with A . Earlier SLAC data on $A/{}^2\text{H}$ ratios [3]) and $A/{}^4\text{He}$ ratios [4] exhibit features similar to those seen by CLAS. The emergence of plateaus is generally interpreted as due to 2- and 3-nucleon short-range correlations in nuclei. However, the physics underlying these correlations has remained elusive. Short-distance multi-quark [5] or multi-nucleon clustering [2, 6, 7] has been favored in several models. See [7, 8] for a review.

In this paper we demonstrate the limited extent to which the observed plateaus can be explained in terms of realistic inter-nucleon potentials including local short-distance repulsion [9, 10], which can push a nucleon momentum to large values. The resulting 2-nucleon (NN) correlations produce a nearly nucleus-independent shape of single nucleon momentum l distributions in the $2 \lesssim l \lesssim 4 \text{ fm}^{-1}$ range [10, 11], which may explain the first plateau. At higher momenta, 3-nucleon (NNN) correlations become dominant [9]. We investigate whether the NNN correlations may explain the second plateau.

Our main theoretical inputs are realistic nuclear wave functions [9, 10], and the collinear factorization framework to describe the scattering of the lepton on a bound nucleon in terms of electron-parton scatterings. The obtained formulas are rather general and the few approximations are made explicit. The formalism is easily generalizable to include other physical mechanisms.

We provide a minimalist approach that includes only the effect of ‘‘Fermi motion’’, or single-nucleon momentum distributions, with exact treatment of kinematics at the parton, nucleon and nuclear level. It provides a baseline, including only nucleon degrees of freedom and the best available nuclear wave-functions. We find that, while the first plateau may be explained in our model, the second plateau in the $2 \lesssim x_B \lesssim 3$ region is not described by inclusion of NNN correlations. Thus, single-

nucleon degrees of freedom are inadequate, and more exotic physical mechanisms such as those mentioned above are needed to explain experimental data.

Collinear factorization. Under the one-photon approximation, the cross section of nuclear deep inelastic scattering is determined by the nuclear hadronic tensor,

$$W_A^{\mu\nu}(p_A, q) = \frac{1}{4\pi} \int d^4z e^{-iq \cdot z} \langle p_A | j^{\dagger\mu}(z) j^\nu(0) | p_A \rangle, \quad (1)$$

with nuclear momentum $P_A = A p_A$, virtual photon momentum q , and corresponding current j . At large Bjorken $x_B = Q^2/2p_A \cdot q$ with $Q^2 = -q^2$, the virtual photon is very localized in space-time. In the impulse approximation, the virtual photon interacts with a parton of momentum k belonging to a nucleon of momentum p , bound in a nucleus of momentum P_A and mass $M_A = A\bar{m}$, as sketched in Fig. 1. We picture the nucleus as a system of A bound nucleons whose momentum distributions (‘‘Fermi motion’’) are given by nuclear many-body wave functions. If we assume the Hilbert space of the nucleus to be the direct product of A single-nucleon Hilbert spaces, and the current operator to act on a single-nucleon subspace,

$$\begin{aligned} W_A^{\mu\nu}(p_A, q) &\approx \int d^4z \frac{1}{4\pi} \int d\mu_A e^{-iq \cdot z} \langle p | j^{\dagger\mu}(z) j^\nu(0) | p \rangle \\ &\equiv \int d\mu_A W_N^{\mu\nu}(p, q), \end{aligned} \quad (2)$$

with $W_N^{\mu\nu}$ the hadronic tensor of a bound nucleon, and relativistic Fermi smearing measure, with $m^2 = p^2$,

$$d\mu_A = \frac{dm^2}{2\pi} \frac{d^3p}{(2\pi)^3 2p_0} \rho_A(p) \Big|_{p_0 = \sqrt{m^2 + \vec{p}^2}}. \quad (3)$$

The single nucleon 4-momentum distribution (ND) is

$$\begin{aligned} \rho_A(p) &= \int \left(\prod_{i=2,A}^A \frac{d^4p'_i}{(2\pi)^4} \right) |\phi_A(p, p'_2, \dots, p'_A)|^2 \\ &\times \delta^{(4)}(p + \sum_{i=2}^A p'_i - A p_A) \end{aligned} \quad (4)$$

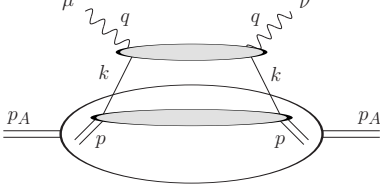


FIG. 1: Forward Compton amplitude for nuclear DIS.

with ϕ_A the nuclear wave-function. Gauge invariance and Eq. (2) imply $q_\mu W_A^{\mu\nu} = q_\mu W_N^{\mu\nu} = 0$, so we can define the nuclear and nucleon structure functions as follows:

$$\begin{aligned} W_A^{\mu\nu}(x_B, Q^2) &= -\tilde{g}^{\mu\nu} F_{1A}(x_B, Q^2) + \frac{\tilde{p}_A^\mu \tilde{p}_A^\nu}{p_A \cdot q} F_{2A}(x_B, Q^2) \\ W_N^{\mu\nu}(x_N, Q^2) &= -\tilde{g}^{\mu\nu} F_1(x_N, Q^2) + \frac{\tilde{p}^\mu \tilde{p}^\nu}{p \cdot q} F_2(x_N, Q^2) \end{aligned} \quad (5)$$

where $x_N = Q^2/2p \cdot q$ and $\tilde{g}^{\mu\nu} = g^{\mu\nu} - q^\mu q^\nu/q^2$, and $\tilde{a}^\mu = a^\mu - (a \cdot q/q^2)q^\mu$ for any 4-vector a .

To evaluate the hadronic tensor or the structure functions in terms of the QCD collinear factorization approach [12], we need to define suitable light-cone “+” and “-” directions. We have 2 choices: using the (q, p_A) plane (A-frame) or using the (q, p) plane (N-frame). Our goal is to express the nuclear structure functions in terms of nucleon structure functions. Hence, as we will discuss, the optimal choice is the N-frame,

$$\begin{aligned} p^\mu &= p^+ \bar{n}^\mu + \frac{m^2}{2p^+} n^\mu \\ q^\mu &= -\xi_A \omega p^+ \bar{n}^\mu + \frac{Q^2}{2\xi_A \omega p^+} n^\mu \\ p_A^\mu &= \omega p^+ \bar{n}^\mu + \frac{\bar{m}_\perp^2}{2\omega p^+} n^\mu + \tilde{p}_{A\perp}^\mu \end{aligned} \quad (6)$$

where $\bar{n} = (1/\sqrt{2}, \vec{0}_\perp, 1/\sqrt{2})$, $n = (1/\sqrt{2}, \vec{0}_\perp, -1/\sqrt{2})$, and $a^\pm = (a_0 \pm a_3)/\sqrt{2}$. In Eq. (6), $\omega = p_A^+/p^+$ is

the inverse nucleon fractional plus-momentum with respect to the nucleus, $\bar{m}_\perp^2 = \bar{m}^2 + p_{A\perp}^2$, and $\xi_A = 2x_B/(1 + \sqrt{1 + 4x_B^2 \bar{m}_\perp^2/Q^2})$ is the nuclear Nachtmann variable [13] in the N-frame.

Following QCD collinear factorization, we expand the parton momentum k , entering the top blob in Fig. 1, around its positive light-cone component, $k^\mu = xp^+ \bar{n}^\mu + O(k - xp^+ \bar{n})$ with parton momentum fraction, $x = k^+/p^+$, and factorize the nucleon hadronic tensor as

$$\begin{aligned} W_N^{\mu\nu}(x_N, Q^2) &= \sum_f \int \frac{dx}{x} \mathcal{H}_f^{\mu\nu}(\bar{x}, Q^2) \varphi_{f/N}(x, Q^2) \\ &+ O(1/Q^2) \end{aligned} \quad (7)$$

where $x_N = \xi_A \omega / (1 - (\xi_A \omega)^2 m^2/Q^2)$ and $\bar{x} = Q^2/2k \cdot q = (\xi_A \omega)/x$ in the N-frame. In Eq. (7), $\varphi_{f/N}$ is the leading twist PDF of a bound off-shell nucleon for a parton of flavor $f = g, q, \bar{q}$, and $\mathcal{H}_f^{\mu\nu}$ is the partonic tensor for an on-shell parton of momentum $k^\mu = xp^+ \bar{n}^\mu$ with all perturbative collinear divergences along the parton momentum k absorbed into the PDFs. With no surprise, Eq. (7) has the same factorized form as that of a free nucleon [14] because the factorization of short-distance partonic dynamics is insensitive to the details of long-distance hadron physics. From the parton level gauge invariance, $q_\mu \mathcal{H}_f^{\mu\nu} = 0$, we can decompose the partonic tensor as

$$\mathcal{H}_f^{\mu\nu}(\bar{x}, Q^2) = -\tilde{g}^{\mu\nu} h_f^1(\bar{x}, Q^2) + \frac{\tilde{k}^\mu \tilde{k}^\nu}{k \cdot q} h_f^2(\bar{x}, Q^2), \quad (8)$$

where the scalar functions h_f^i can be computed order-by-order in powers of α_s from the factorized expression (7) with the nucleon state N replaced by a parton state of flavor f , regardless of the nucleon state.

Combining Eqs. (2), (5), (7) and (8) we derive nuclear structure functions in terms of leading twist massless ($m^2 = 0$) nucleon structure functions, $F_i^{(0)}$ with $i = 1, 2$

$$F_{2A}(x_B, Q^2) = \frac{x_B}{1 + \delta_A} \int d\mu_A \left[\frac{3(1 + \delta_\omega)^2}{(1 + \delta_A)(1 + \delta_n)} - 1 \right] \frac{F_2^{(0)}(\xi_A \omega, Q^2)}{2\xi_A \omega} \theta(1 - \xi_A \omega) \quad (9)$$

$$F_{1A}(x_B, Q^2) = \int d\mu_A \left\{ F_1^{(0)}(\xi_A \omega, Q^2) + \left[\frac{(1 + \delta_\omega)^2}{(1 + \delta_A)(1 + \delta_n)} - 1 \right] \frac{F_2^{(0)}(\xi_A \omega, Q^2)}{4\xi_A \omega} \right\} \theta(1 - \xi_A \omega) \quad (10)$$

where $\delta_A = 4x_B^2 \bar{m}^2/Q^2$, $\delta_n = 4x_N^2 m^2/Q^2$, $\delta_\omega = 4x_B x_N M_\omega^2/Q^2$, and $M_\omega^2 = \frac{\omega}{2} [m^2 + \bar{m}_\perp^2/\omega^2]$.

We would like to emphasize that only in the N-frame we can easily generalize the free-nucleon PDF to the PDF of a bound off-shell nucleon because they both have the same operator definition. For example, other than the

state $|p\rangle$, the definition of quark PDF at leading order,

$$\varphi_q(x) = \int \frac{dz^-}{2\pi} e^{-ixp^+ z^-} \langle p | \bar{\psi}(z^- n) \frac{\gamma^+}{2} \psi(0) | p \rangle \quad (11)$$

is the same for both bound and free nucleon [15]. This would not be true in the A-frame.

Large- x_B correlations. To apply the general result, Eqs. (9)-(10), to describe CLAS data we need to choose $F_i^{(0)}$ of bound nucleons and the measure $d\mu_A$. First, we assume the nucleons to be on their mass-shell with $m^2 = \bar{m}^2$. Thus, we may identify $F_i^{(0)}$ with the massless free nucleon structure functions. They can be computed using PDFs from QCD global fits which do not already correct for the target's mass. Corrections for off-shell nucleons were discussed in Ref. [16] in a related, but somewhat different, formalism. Next, we use non-relativistic computations of nucleon distribution functions [9, 10] (we are not aware of any relativistic model which includes NN and NNN correlations). In summary we approximate

$$\rho_A(p) \approx (2\pi)^4 2p_0 \delta(p^2 - \bar{m}^2) \rho_A^{nr}(\vec{p}). \quad (12)$$

Defining $p_A = p + l$, using the translation invariance of the nucleon distribution, and choosing the struck nucleon rest frame, $p = (m, \vec{0})$, we obtain $d\mu_A = d^3l \rho_A^*(\vec{l})$, where $\rho_A^*(l) = \int (\prod_{i=2,A}^A d^3l_i) |\phi_A(l, l_2, \dots, l_A)|^2 \delta^{(3)}(l + \sum_{i=2}^A l_i)$ can be identified with the nucleon distribution computed in the nucleus rest frame. We consider state-of-the-art non-relativistic nucleon distribution functions ρ_A^* obtained in a Variational Monte Carlo (VMC) computation which include NN and NNN correlations [9], compared to the parametrization of ρ_A^* discussed by Ciofi degli Atti and Simula (CS) [10], which only considers NN correlations, see Fig. 2. The relative momentum $\vec{l} = (\vec{l}_\perp, l_3)$ further enters Eq. (9) through $\omega = (l_3 + \sqrt{l_\perp^2 + \bar{m}_\perp^2})/m$ and $\bar{m}_\perp^2 = \bar{m}^2 + l_\perp^2$. The per-nucleon nuclear deep inelastic (DIS) cross section reads

$$\frac{d\sigma_A}{dQ^2 dx_B} = \frac{4\pi\alpha^2}{Q^4} \left\{ \frac{1}{A} y^2 F_{1A}(x_B) + \left(1 - y - \frac{\bar{m}^2}{Q^2} x_B^2 y^2 \right) \frac{F_{2A}(x_B)}{x_B} \right\} \quad (13)$$

where $y = P_A \cdot q / P_A \cdot p_l = Q^2 / (2E_{lab} \bar{m} x_B)$, p_l is the lepton initial 4-momentum and E_{lab} its energy in the target rest frame. The nuclear structure functions F_{iA} are given in Eqs. (9)-(10). For the following plots, we compute $F_i^{(0)}$ at leading order using CTEQ5L PDF [17].

In Fig. 3 left, we compare the $A/{}^3He$ ratios from Eq.(13) with CLAS data taken at $Q^2 \sim 2 \text{ GeV}^2$ [1]. After an initial rise, the computed ratio becomes softer starting at $x_B \gtrsim 1.5$. This is due to the onset of NN correlations which develop a tail in the nucleon distribution at $|l| \gtrsim 2 \text{ fm}^{-1}$, see Fig. 2. Our curves using VMC distributions (solid lines) can describe reasonably well CLAS data for light nuclei. However, they do not describe the onset of the second plateau, otherwise visible in the ND ratios of Fig. 2 and due to the onset of NNN correlations. Indeed, in the Fermi smearing of the structure functions (9)-(10), the nucleon momentum l is sampled with a rather large standard deviation of about 1 fm^{-1} , which smears out such structure. This second plateau

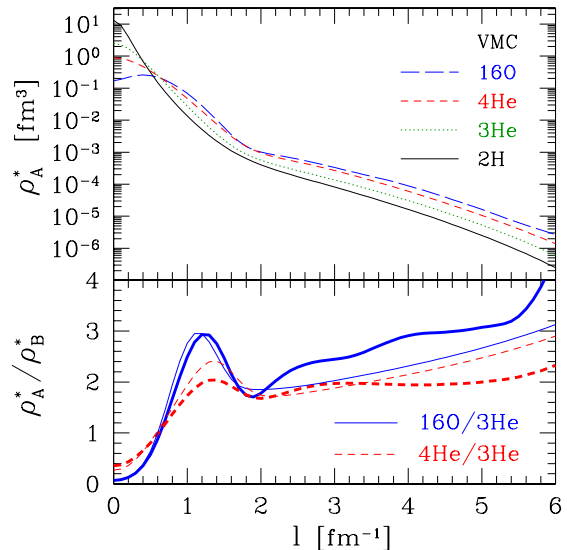


FIG. 2: Top: VMC nucleon momentum distributions [9]. Bottom: $A/{}^3He$ ratios (thick: VMC; thin: CS [10]).

is then suggestive of new mechanisms such as 6- and 9-quark clusters [5], multi-nucleon clusters [2, 6, 7], or dynamical short-range nucleon correlations [18], effective when nucleons approach each other at a distance smaller than a nucleon radius. In light nuclei such as 3He or 4He , all nucleons exist on the nuclear surface, which reduces the probability of nucleon overlap. In heavier nuclei, an increasing fraction of nucleons exist in the nuclear interior where the overlap probability is maximized, so that we expect the difference between our baseline and experimental data to increase with A at $x > 2.25$. The computation with the CS distributions (dashed lines) fails at $x_B \gtrsim 1.5$ for nuclei heavier than 4He , perhaps due to the lack of NNN correlations.

In Fig. 3 right, we show the effect of Fermi motion on $A/{}^3He$ ratios at $Q^2 = 5 \text{ GeV}^2$. The onset of correlation effects has moved down to $x_B \sim 1$ and the plateau's slope has increased. At still higher values of Q^2 we found that the onset of correlation effects does not move much further, but the slope of the plateau continues to increase.

We estimated the sensitivity of the A/B ratios to different choices of PDF, which is at most 5%. Parton recombination effects, which are important at small- x_B [19], are negligible in our case.

The simple model of the nucleus we have considered can be improved in many ways. First, we used a non-relativistic computation of ρ_A to describe the large x_B region, to which nucleons of relative momentum $l \gtrsim 2 \text{ fm}^{-1}$ contribute: one may expect relativistic corrections to become important and change the hard tails of the ND. Second, the nucleon hadronic tensor can have a more general Lorentz decomposition than in Eq. (5), as discussed in [16] where our assumption leading to Eq. (2) was relaxed. Finally, we have made no attempt to describe the EMC

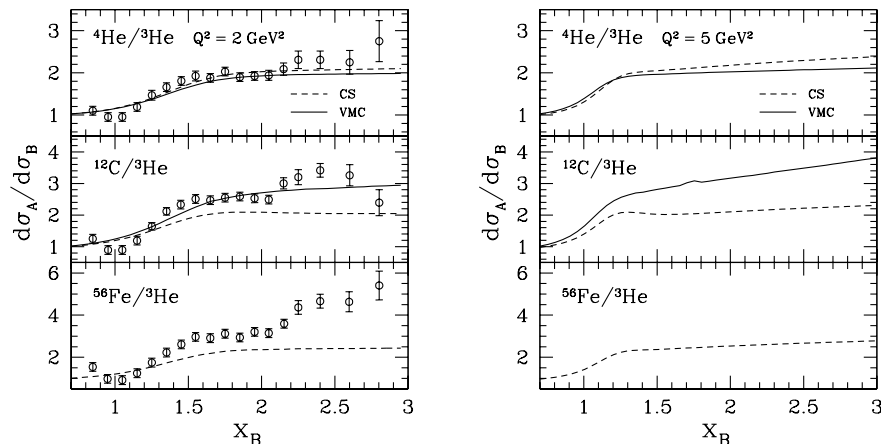


FIG. 3: Left: Comparison of cross-section ratios computed at $Q^2 = 2 \text{ GeV}^2$ and $E_{lab} = 4.5 \text{ GeV}$ to CLAS data taken at $1.6 \text{ GeV}^2 < Q^2 < 2.4 \text{ GeV}^2$ [1]. Solid line computed with VMC nucleon distributions [9], dashed line with the CS parametrization [10]. Right: cross-section ratios at $Q^2 = 5 \text{ GeV}^2$ and $E_{lab} = 9 \text{ GeV}$, accessible at the 12 GeV upgrade at JLAB.

effect in the $0.2 \lesssim x_B \lesssim 1$ region, see [20, 21] for a review. Proposed underlying mechanisms include off-shell corrections to nucleon structure functions, nucleon binding and removal energy corrections, and Q^2 -rescaling. Their impact at large- x_B needs to be estimated, but we do not expect major changes to our results since the cross-section ratios at large x_B are mainly dominated by the relative strength of the ND tails. Quasi-elastic lepton-nucleon scattering, which causes the dip in experimental data at $x_B \approx 1$ can be straightforwardly implemented, as well as contributions from the nuclear pionic cloud. However, such improvements are not expected to make significant contributions at large x_B .

Finally, at the lower Q^2 we considered, a few theoretical issues arise. First, especially at $Q^2 \approx 2 \text{ GeV}^2$, one can question the partonic picture of DIS for computing F_{2A} . When computing the ratio, however, this should not be an issue thanks to parton hadron duality. Second, one would expect higher-twist corrections to become sizable. They would not completely cancel in the ratio, because they are expected to be proportional to $A^{1/3}$. We will consider these issues in a future work, but we expect these improvements to provide cross section ratios with smooth corrections that will not likely induce the second plateau structure seen in the CLAS data.

We thank G. Miller and S. C. Pieper for informative discussions, and INT Seattle and BNL for hospitality. We acknowledge support from DOE grant DE-FG02-87ER40371 and Contract No. DE-AC02-98CH10886.

- [2] K. S. Egiyan *et al.* [CLAS], Phys. Rev. C **68** (2003) 014313.
- [3] L. L. Frankfurt, M. I. Strikman, D. B. Day and M. Sargsian, Phys. Rev. C **48** (1993) 2451, and references therein.
- [4] D. Day, Nucl. Phys. A **478** (1988) 397C.
- [5] H. J. Pirner and J. P. Vary, Phys. Rev. Lett. **46** (1981) 1376; M. Sato, S. A. Coon, H. J. Pirner and J. P. Vary, Phys. Rev. C **33** (1986) 1062. G. Yen, J. P. Vary, A. Harindranath and H. J. Pirner, Phys. Rev. C **42** (1990) 1665.
- [6] L. L. Frankfurt and M. I. Strikman, Phys. Rept. **76** (1981) 215.
- [7] L. L. Frankfurt and M. I. Strikman, Phys. Rept. **160** (1988) 235.
- [8] M. M. Sargsian *et al.*, J. Phys. G **29** (2003) R1.
- [9] S. C. Pieper, R. B. Wiringa and V. R. Pandharipande, Phys. Rev. C **46** (1992) 1741.
- [10] C. Ciofi degli Atti and S. Simula, Phys. Rev. C **53** (1996) 1689.
- [11] J. G. Zabolitzky and W. Ey, Phys. Lett. B **76**(1978) 527.
- [12] J. C. Collins, D. E. Soper and G. Sterman, Adv. Ser. Direct. High Energy Phys. **5** (1988) 1.
- [13] O. Nachtmann, Nucl. Phys. B **63** (1973) 237; P. H. Frampton, Lett. Nuovo Cim. **17** (1976) 499.
- [14] G. Curci, W. Furmanski and R. Petronzio, Nucl. Phys. B **175** (1980) 27.
- [15] J. C. Collins and D. E. Soper, Nucl. Phys. B **194** (1982) 445.
- [16] W. Melnitchouk, A. W. Schreiber and A. W. Thomas, Phys. Rev. D **49** (1994) 1183.
- [17] H. L. Lai *et al.*, Eur. Phys. J. C **12** (2000) 375.
- [18] E. Piasetzky, M. Sargsian, L. Frankfurt, M. Strikman and J. W. Watson, Phys. Rev. Lett. **97** (2006) 162504
- [19] F. E. Close, J. W. Qiu and R. G. Roberts, Phys. Rev. D **40** (1989) 2820.
- [20] P. R. Norton, Rept. Prog. Phys. **66** (2003) 1253.
- [21] G. Piller and W. Weise, Phys. Rept. **330** (2000) 1.

[1] K. S. Egiyan *et al.* [CLAS], Phys. Rev. Lett. **96** (2006) 082501.